Experimental section

Materials: Isopropyl chloroformate, and 4-aminobenzyl cyanide were purchased from Alfa Aesar Co. Ltd. Other reagents were obtained from Sigma-Aldrich or Aladdin Chemicals and used without further purification. Solvents were purified according to standard laboratory methods.

Instrumentation: ^{1}H NMR and ^{13}C NMR of correlative derivatives were recorded on a Brüker AM500 spectrometer using Tetramethyl silane (TMS, δ=0 ppm) as internal standard. The Time-resolved PL decay spectra of the samples were also performed on an Edinburgh FLS980 fluorescence spectrometer at room temperature. PL measurements at room temperature were obtained on a SENS-9000 (Gilden Photonics, England). The digital photo-graphs were captured by the 550D digital cameras (Canon, Japan). Absolute PL quantum yields (**PLQYs**) were determined with a spectrometer C11347 (Hamamatsu, Japan). Powder X-ray diffraction experiments were measured on a Philips X'Pert Pro diffractometer (Netherlands). Measurements were made in a 2θ range of 5-45° at room temperature with a step of 0.02° (2θ). The scan speed was 2 degree/min. The UV-vis absorption spectra were obtained on a Shimadzu UV-2600 spectrophotometer (Japan). Single crystal X-ray diffraction data were collected on a Rigaku R-AXIS RAPID diffractometer using the ω-scan mode with graphite-monochromator Mo·Kα radiation. The structures were solved with direct methods using the SHELXTL programs and refined with full-matrix least-squares on F^2.

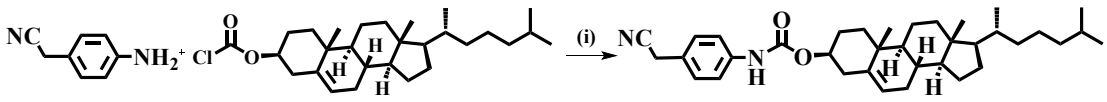

BCN

Synthesis of the intermediate compound **BCN**. Cholesteryl chloroformate (2.69 g, 6.0 mmol) was dissolved in dry THF (20 mL), and the solution was added dropwise to the dry THF (30 mL) solution consisting of 2-(4-aminophenyl)acetonitrile (0.66 g, 5.0 mmol) and triethylamine (2.10 mL, 15 mmol) at 0 °C. After stirring at room temperature for 12 h, the solution was poured into water and the product was extracted with $CHCl_3/C_2H_5OH$ at volume ratio of 1:3, and dried in a vacuum. The resulting precipitate was filtered and purified by column chromatography using ethyl acetate/petroleum ether. BCN bulk powder was purified by the recrystallization from $CHCl_3$ and methanol solution. ^{1}H NMR (500 MHz, $CDCl_3$): δ (ppm) 7.41(*d*, J = 8.35 Hz, 2H); 7.26 (d, J = 8.65 Hz, 2H); 6.63(s, 1H); 5.42 (*t*, J = 2.55Hz, 1H); 4.64-4.60(m, 1H); 3.72(s, 2H); 2.43-2.36 (*m*, 2H); 2.02-1.89(*m*, 5H); 1.60-1.53 (*m*, 7H); 1.36-1.35 (*m*, 4H); 1.18-1.10 (*m*, 7H); 1.04(*s*, 3H); 1.03-0.99 (*m*, 3H); 0.93(*d*, J = 6.50 Hz, 3H); 0.88 (*d*, J = 4.45 Hz, 6H); 0.70 (s, 3H). ^{13}C NMR (125 MHz, $CDCl_3$): δ (ppm) 152.90; 139.50; 138.02; 128.62; 124.41; 122.85; 119.04; 117.88; 75.18; 56.69; 56.16; 50.03; 42.33; 39.74; 39.52; 38.43; 36.96; 36.58; 36.19; 35.79; 31.91; 31.88; 28.22; 28.08; 28.00; 24.28; 23.84; 23.00; 22.80; 22.55; 21.05; 19.32; 18.72; 11.86. MS (ESI) m/z: $[M+NH_4]^+$ calcd for $C_{36}H_{52}N_2O_2$, 544.4; found, 562.4.

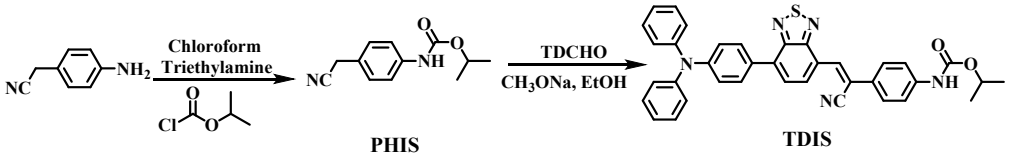

PHIS TDIS

Synthesis of PHIS: Isopropyl chloroformate (1.22 g, 10mmol) in dry chloroform (50 ml) was added at 0-5 °C with vigorous stirring to a solution of 4-aminobenzyl cyanide (1.32 g, 10 mmol) and triethylamine (1.01g, 10 mmol) in the same solvent (50 mL) under dry N_2, over 20 min with cooling. After 1h further, the mixture was warmed to room temperature and left overnight to give a homogenous mixture. The solution was then washed with dilute HCl (10 mL), H_2O(50 mL), dried (Na_2SO_4) and

evaporated in vacuo to give a yellow solid (1.41 g), which was purified further by chromatography on silica with EtOAc/PE as the eluent. Yield 1.13g(51.8%).

^{1}H NMR (400 MHz, $CDCl_3$) δ 7.42 (d, *J* =8 Hz, 2H), 7.27 (d, 2H), 6.66 (s, 1H), 5.07-4.99 (*m*, 1H), 3.72 (*s*, 2H), 1.32 (d, *J* =8 Hz, 2H);^{13}C NMR (100 MHz, $CDCl_3$) δ = 153.22, 138.11, 128.59, 124.36, 119.12, 118.04, 68.94, 22.98, 22.08; HRMS (ESI, m/z): Calcd for $C_{12}H_{15}N_2O_2$: 219.1134 $[M]^+$; Found: 219.1127; m.p.: 187.7 °C

Synthesis of TDIS: The mixture of **TDCHO** (0.407g, 1mmol) and PhIS (0.259g, 1.2mmol) in dry ethanol (30 mL) was stirred for 5 min. And then, a small amount of CH_3ONa were added, and stirred for 18 hours at the room temperature. The desired target product TDIS was filtered and washed with EtOH three times to give deep red powder (0.473g, 78%).

^{1}H NMR (400 MHz, $CDCl_3$) δ 8.72 (d, *J* =7.6 Hz, 1H), 8.5 (s, 1H), 7.94(d, *J* =8.4 Hz, 2H), 7.84 (d, *J* =7.6 Hz, 1H), 7.79 (d, *J* =8.8 Hz, 2H), 7.55 (d, *J* =8.8 Hz, 2H), 7.33 (t, *J* =8.4 Hz, 4H), 7.21-7.24 (m, 6H), 7.11 (*t*, *J* =7.2 Hz, 2H), 6.71 (s, 1H), 5.11-5.06 (m, 1H), 1.35 (d, *J* =6.4 Hz, 6H);^{13}C NMR (100 MHz, $CDCl_3$) δ = 155.06, 153.12, 152.86, 148.67, 147.24, 139.48, 135.38, 133.88, 130.11, 129.90, 129.43, 128.93, 127.88, 127.06, 126.92, 125.18, 125.03, 123.64, 122.37, 118.66, 118.15, 112.07, 69.21, 22.10; HRMS (ESI, m/z): Calcd for $C_{37}H_{30}N_5O_2S$: 608.2120 $[M+H]^+$; Found: 608.2109; m.p.: 187.7 °C

Table S1 Crystal data and structure refinement for crystals **TDCH** and **TDIS**.

Samples	TDCH (CCDC: 2150504)	TDIS (CCDC: 2150513)
Formula	$C_{65}H_{75}N_5O_3S$	$C_{37}H_{29}N_5O_2S$
Mr	1006.36	607.71
Temperature (K)	150.0	170.0
Crystal system	triclinic	monoclinic
Space group	P1	C2/c
Crystal size (mm)	0.12 × 0.08 × 0.05	0.15 × 0.08 × 0.05
a (Å)	10.1099(2)	22.881(3)
b (Å)	12.6710(3)	7.8734(9)
c (Å)	22.5816(5)	35.026(4)
α (°)	77.0490(10)	90
β (°)	79.9500(10)	103.060(7)
γ (°)	89.7300(10)	90
V(Å^3)	2774.13(11)	6146.6(13)
Z	2	8
D_{calc} (mg/m^3)	1.205	1.313
Theta Range (°)	4.08 ~ 149.332	4.776 ~ 52.812
F (000)	1080.0	2544.0
h, *k*, l_{max}	12,15,28	28,9,43
N_{ref}	100088	6303
T_{min}, T_{max}	0.916,0.955	0.986,0.993
Independent reflections	21184	6271
Goodness-of-fit on F^2	1.027	1.055
R_{int}	0.0357	0.0600
$R_1[I>2\sigma(I)]$	0.0458	0.0500
$wR_2[I>2\sigma(I)]$	0.1186	0.1227
R_1(all data)	0.0494	0.0797
wR_2(all data)	0.1228	0.1429
S	1.027	1.055

$R_1 = \Sigma||F_o| - |F_c||/\Sigma|F_o|$, $wR_2 = [\Sigma w(F_o^2 - F_c^2)^2/\Sigma w(F_o^2)^2]^{1/2}$

The change in magnitude of the dipole moment between the ground and excited states, that is, $\Delta\mu = \lfloor \mu_e - \mu_g \rfloor$ can be estimated using the Lippert–Mataga equation

$$hc(v_a - v_f) = hc\left(v_a^0 - v_f^0\right) + \frac{2(\mu_e - \mu_e)^2}{a_0^3} f(\varepsilon,n)$$

Where a_0 is the cavity radius in which the solute resides, estimated to be 9.7 Å. μ_g is the ground-state dipole moment, estimated to be 3.4 D (ωB97X at the basis set level of 6-31G**), μ_e is the excited state dipole moment. h and c are Planck's constant and the speed of light, respectively, and f(ε, n)is the orientation polarizability, defined as

$$f(\varepsilon,n) = \frac{\varepsilon - 1}{2\varepsilon + 1} - \frac{n^2 - 1}{2n^2 - 1}$$

Where ε is the static dielectric constant and n is the optical refractivity index of the solvent. Through the analysis of the fitted line in low-polarity solvents, its corresponding μ_e was calculated to be 11.1 D according to Lippert-Mataga equation. However, in high-polarity solvents, the μ_e was increased to 19.2 D.

Table S2 Detailed photo-physical data of **TDCH** in the different solvents

Solvents	f	λ_{abs} nm	λ_{flu} nm	ν_a cm^{-1}	ν_f cm^{-1}	ν_a-ν_f cm^{-1}	PLQYs
Hexane	0.0012	488	568	20492	17606	2886	99.5%
Toluene	0.014	492	610	20325	16393	3932	95.6%
Butyl ether	0.096	489	610	20450	16393	4056	88.9%
Isopropyl ether	0.145	487	612	20534	16340	4194	91.3%
Ethyl ether	0.167	485	620	20619	16129	4490	91.5%
THF	0.210	485	658	20619	15198	5421	59.3%
DCM	0.217	485	674	20619	14836	5783	56.3%
DMF	0.276	481	722	20790	13850	6940	2.7%
Acetone	0.284	477	690	20964	14493	6472	8.1%
Acetonitrile	0.305	470	708	21277	14124	7152	2.6%

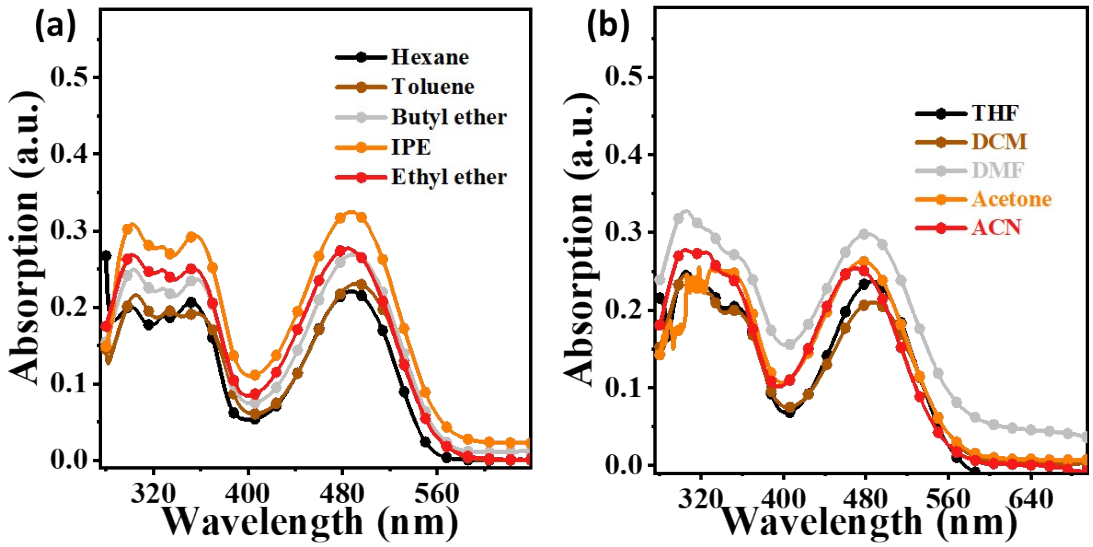

Fig. S1 The UV absorption spectra of **TDCH**, measured in the different solvents with increasing polarity (the orientational polarizability of solvent, Δ*f*, –hexane: 0.0012; toluene: 0.014; butyl ether: 0.096; isopropyl ether (IPE): 0.145; ethyl ether: 0.167; tetrahydrofuran (THF): 0.210; methylene chloride (DCM): 0.217; N,N-dimethylformamide (DMF): 0.276; Acetone: 0.284; and acetonitrile (ACN): 0.305).

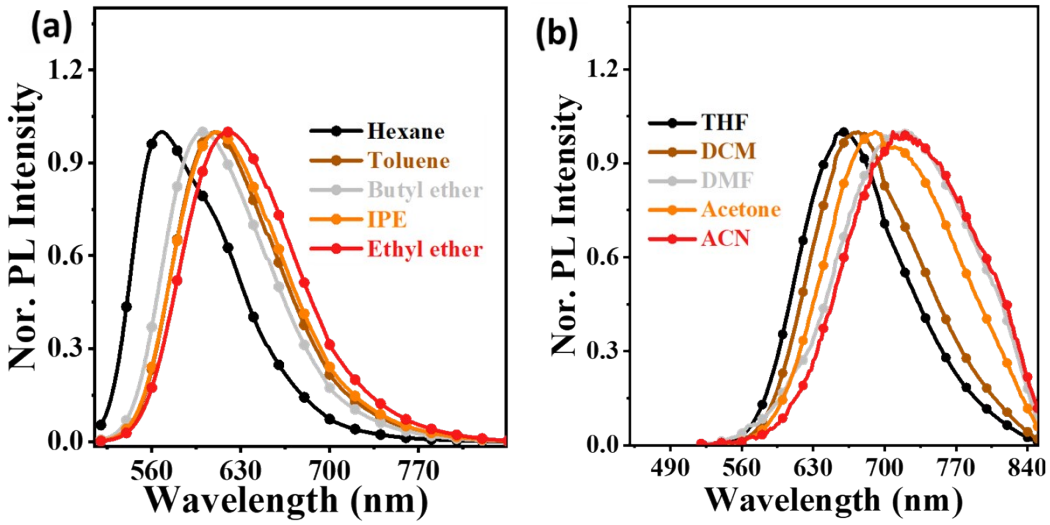

Fig. S2 PL spectra of **TDCH** in the different solvents (the orientational polarizability, Δ*f*, –hexane: 0.0012; toluene: 0.014; butyl ether: 0.096; isopropyl ether (IPE): 0.145; ethyl ether: 0.167; tetrahydrofuran (THF): 0.210; methylene chloride (DCM): 0.217; N,N-dimethylformamide (DMF): 0.276; Acetone: 0.284; and acetonitrile (ACN): 0.305).), the excitation wavelength is 450 nm.

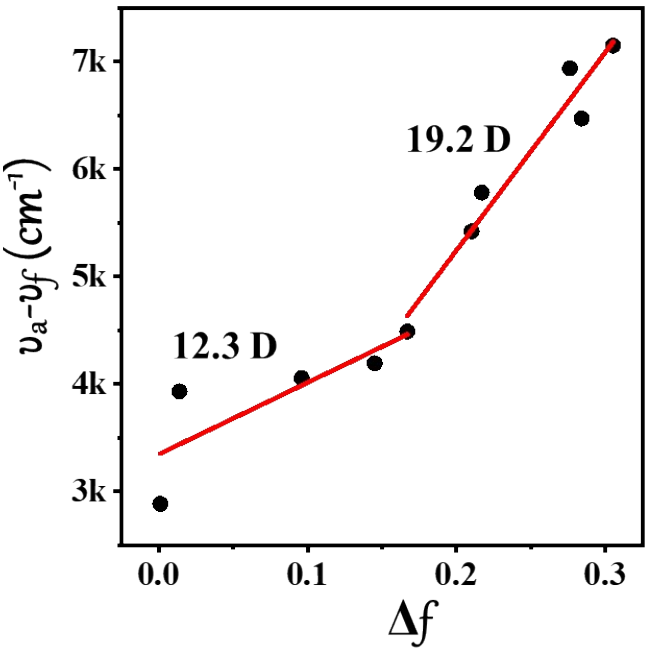

Fig. S3 Linear fitting of orientation polarization (Δf) of the solvent media with the Stokes shift (υ_a–υ_f) for **TDCH** (the detailed data are listed in Table S2, Supporting Information);

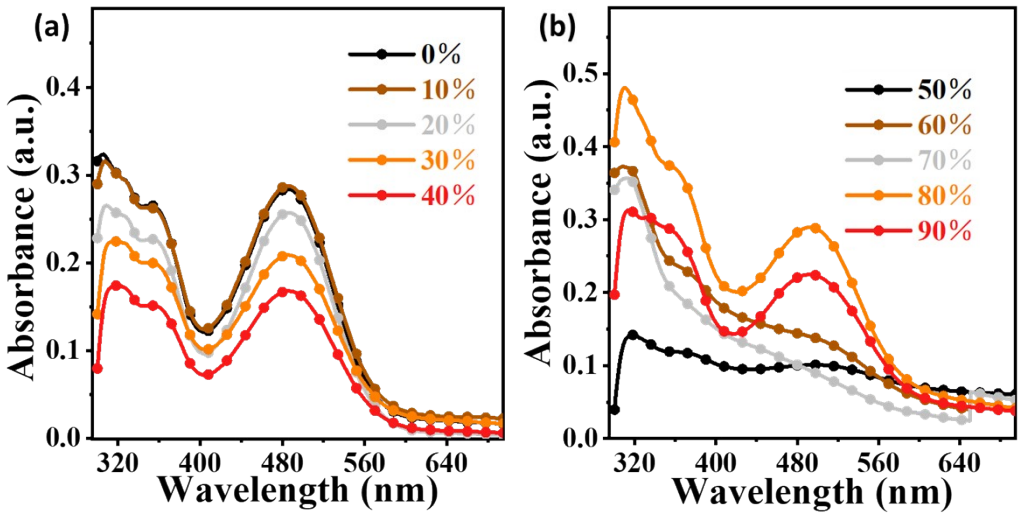

Fig. S4 a,b)The UV absorption spectra of **TDCH** (10 μM) in THF/water mixtures with different water fractions (f_w). The absorption spectra of the luminophor in THF and in mixtures of less than 50% H_2O with THF were almost identical. However, above 50% volume fraction (fw) of water, the absorption bands became more intense and moved to longer wavelengths. Moreover, tailing was clearly observed in visible region, and this absorption was due to the presence of nanoparticle suspensions.

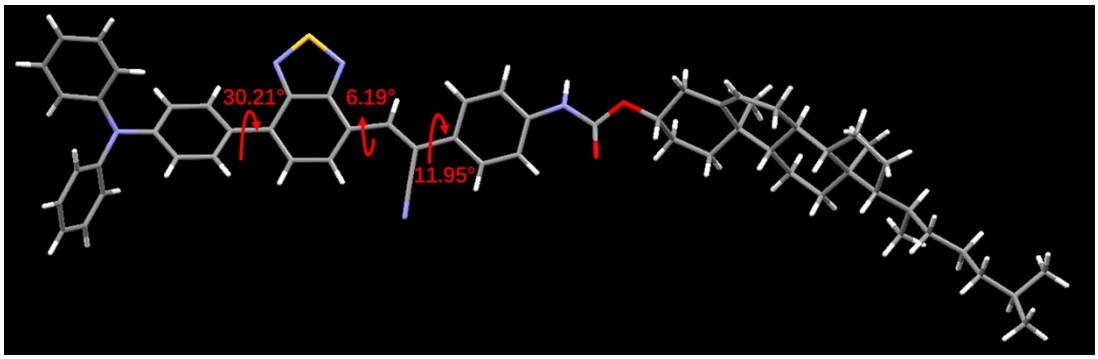

Fig. S5 Dihedral angles between acrylonitrile and **BTA** as well as benzene units

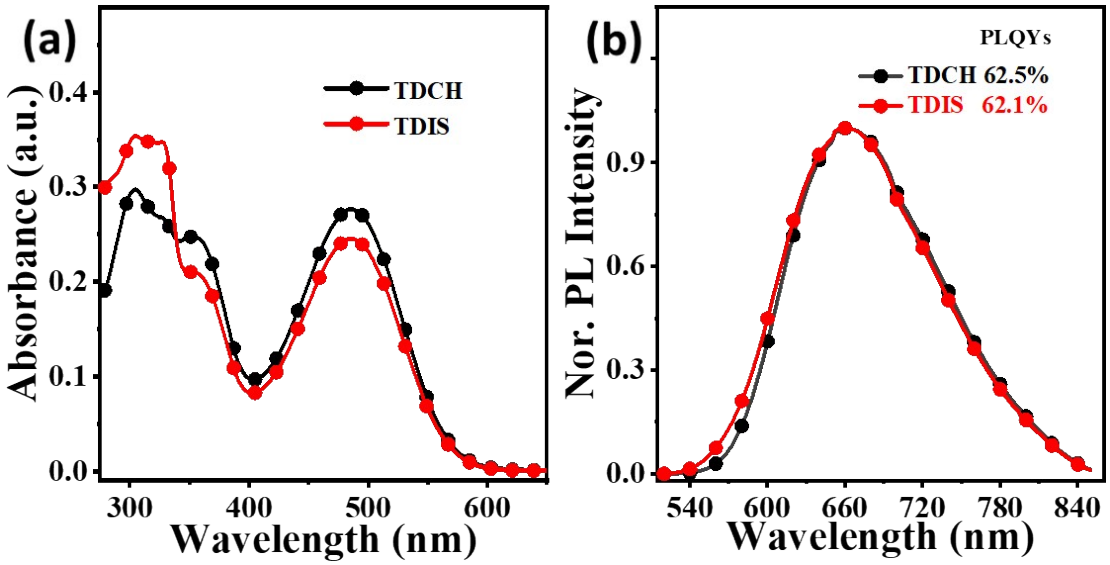

Fig. S6 The UV absorption spectra (a) and PL spectra (b) of **TDCH** and **TDIS** in THF (10 μM)

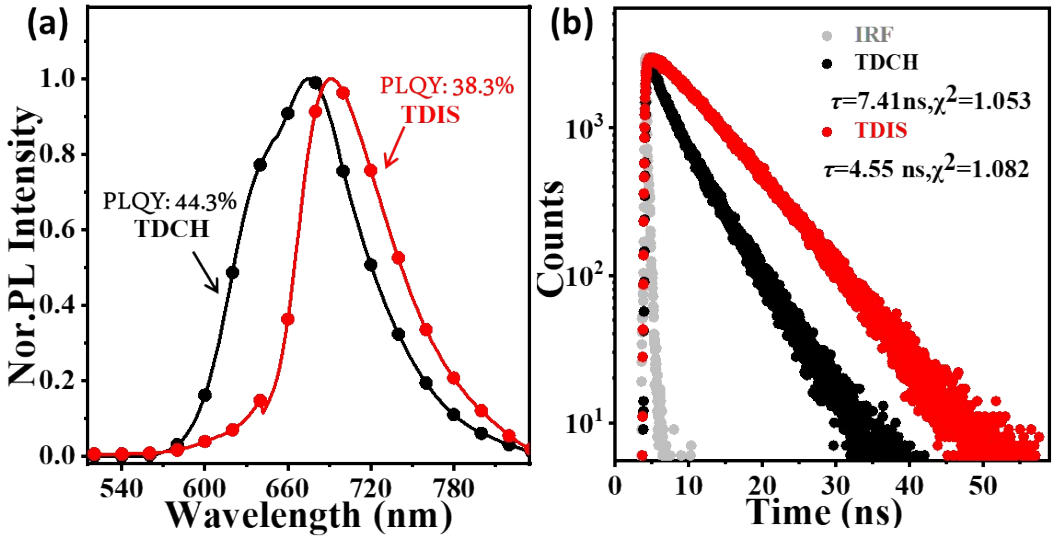

Fig. S7 (a) Steady-state PL spectra and (b) Time-resolved PL decay curves of **TDCH** and **TDIS** crystalline powder.

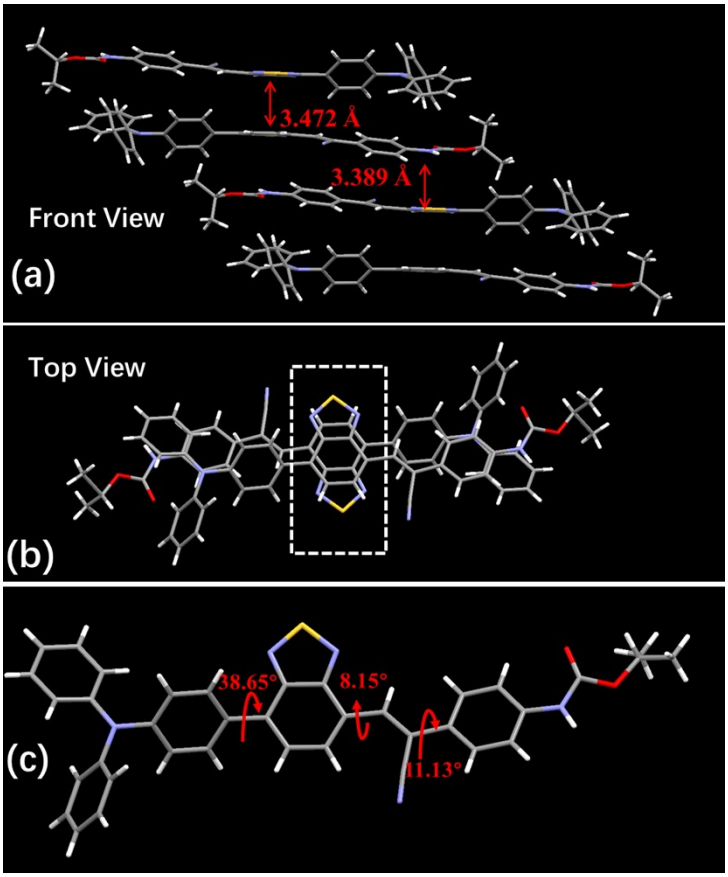

Fig. S8 Crystal structures of **TDIS**: (a) Lateral view of the column arrangement; (b) top view of the **TDIS**; (c) and the dihedral angles of the **TDIS** single-crystal.

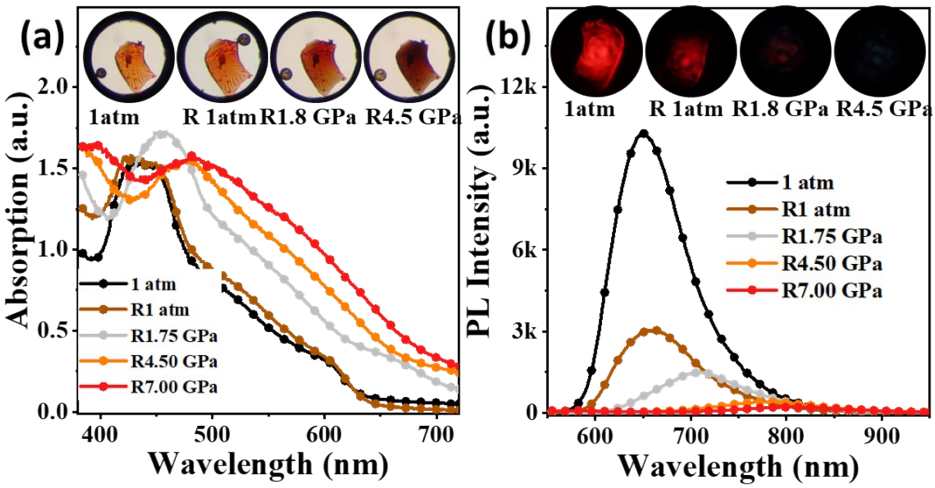

Fig. S9 The UV absorption spectra (a) and PL spectra (b) of **TDCH** crystals during the depressurizing process.

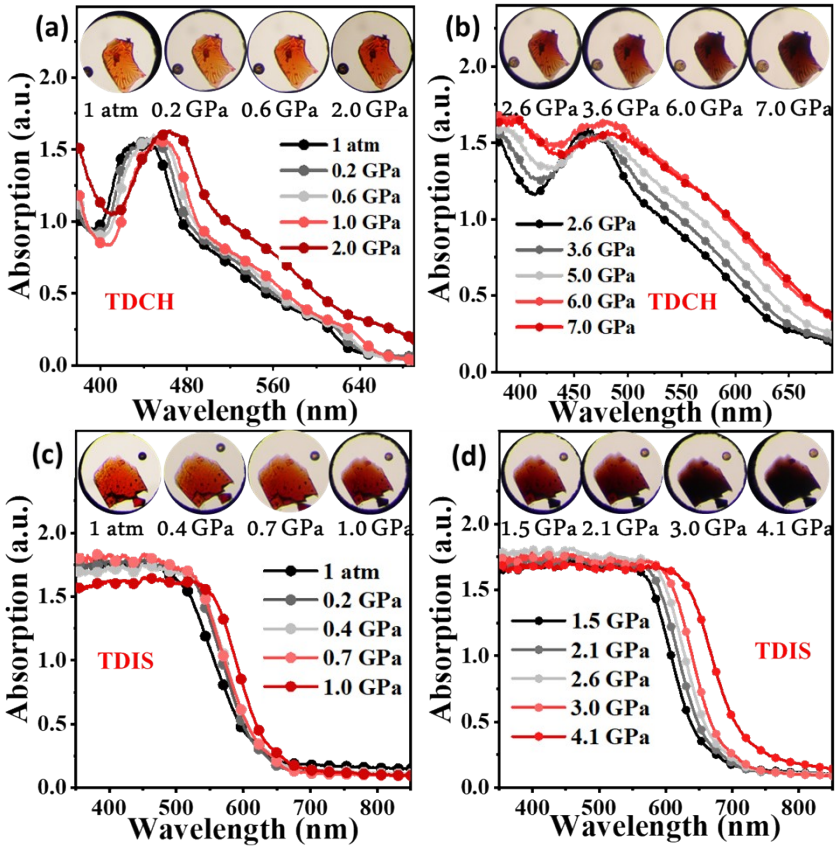

Fig. S10 Absorption spectra of **TDCH** (a, b) and **TDIS** (c, d) crystalline powders under different hydrostatic pressures.

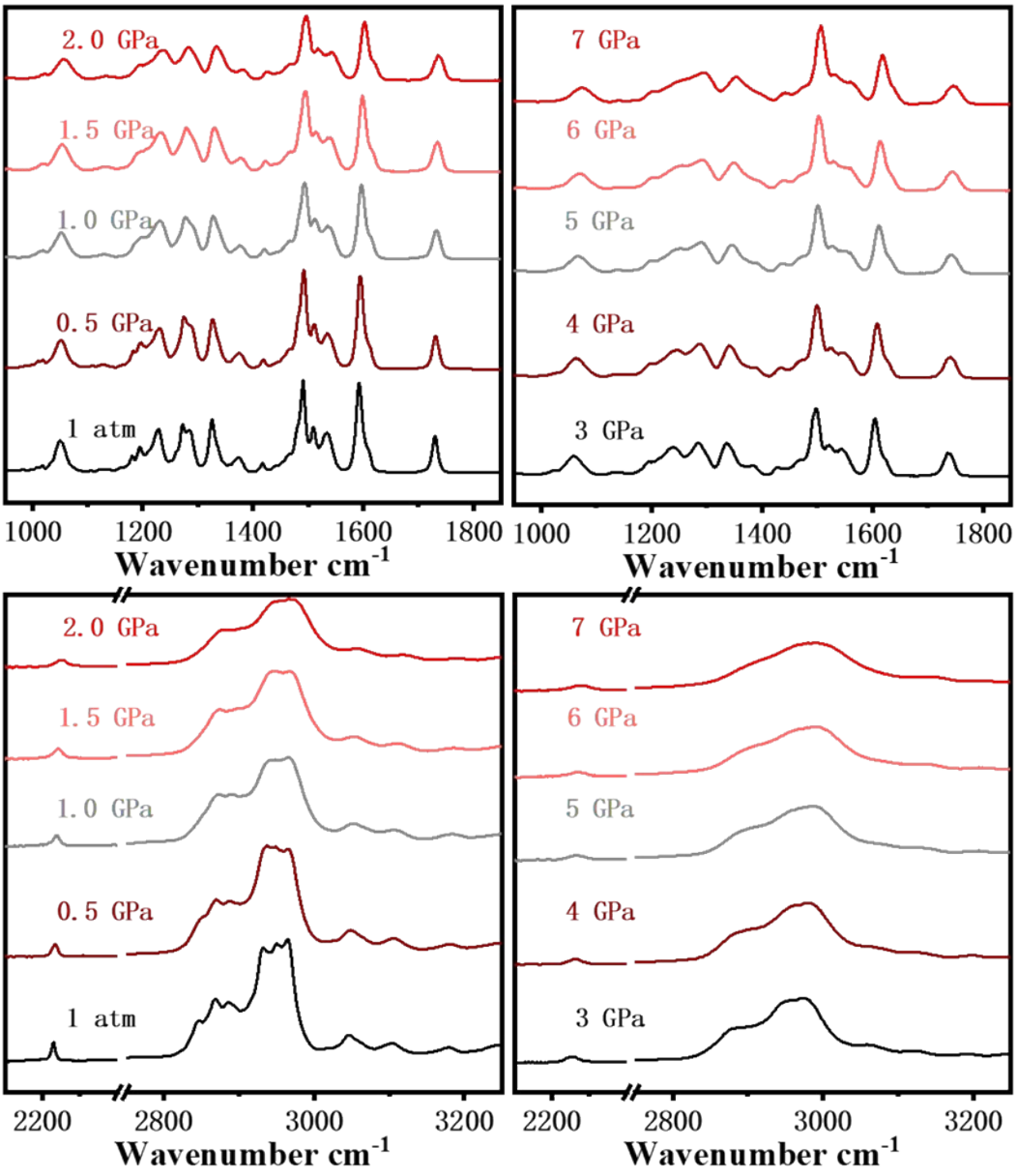

Fig. S11 IR spectra of **TDCH** crystals in the range of 1000-3200 cm^{-1} at various pressures

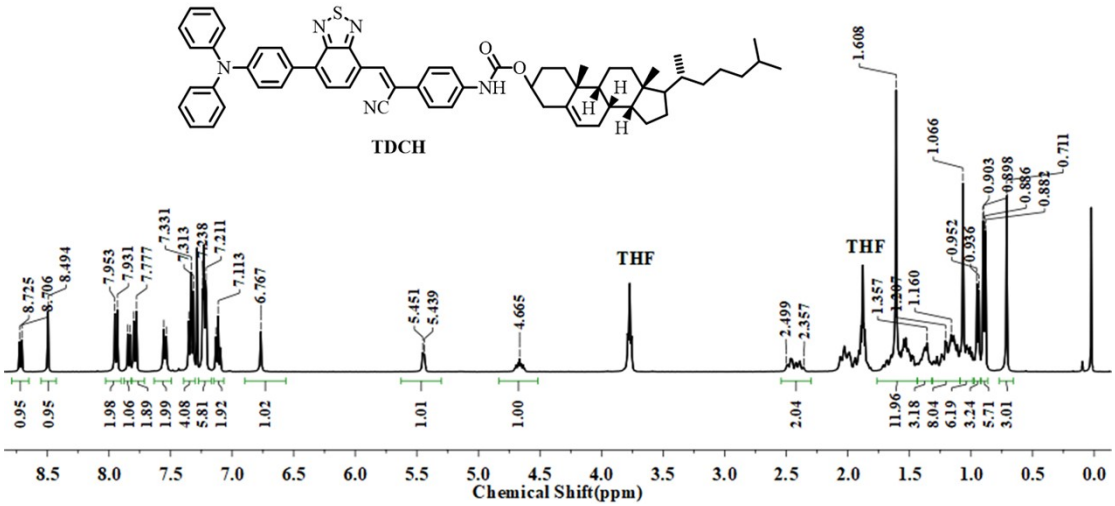

Fig. S12 The ^{1}H NMR spectrum of **TDCH** in the $CDCl_3$.

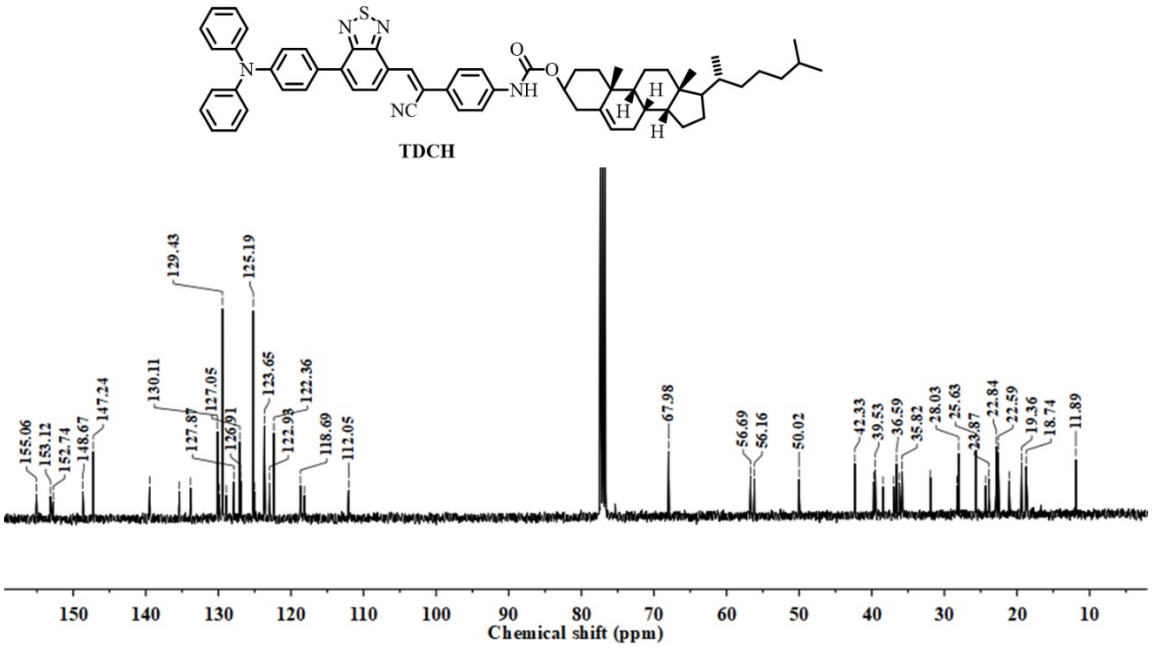

Fig. S13 The ^{13}C NMR spectrum of the **TDCH** in the $CDCl_3$.

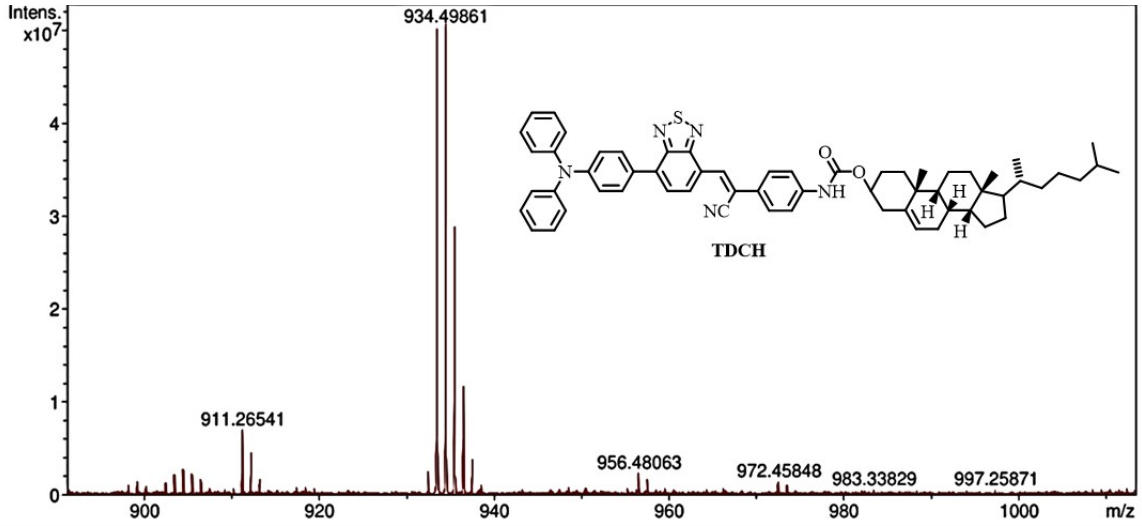

Fig. S14 The HRMS spectrum of the **TDCH**.

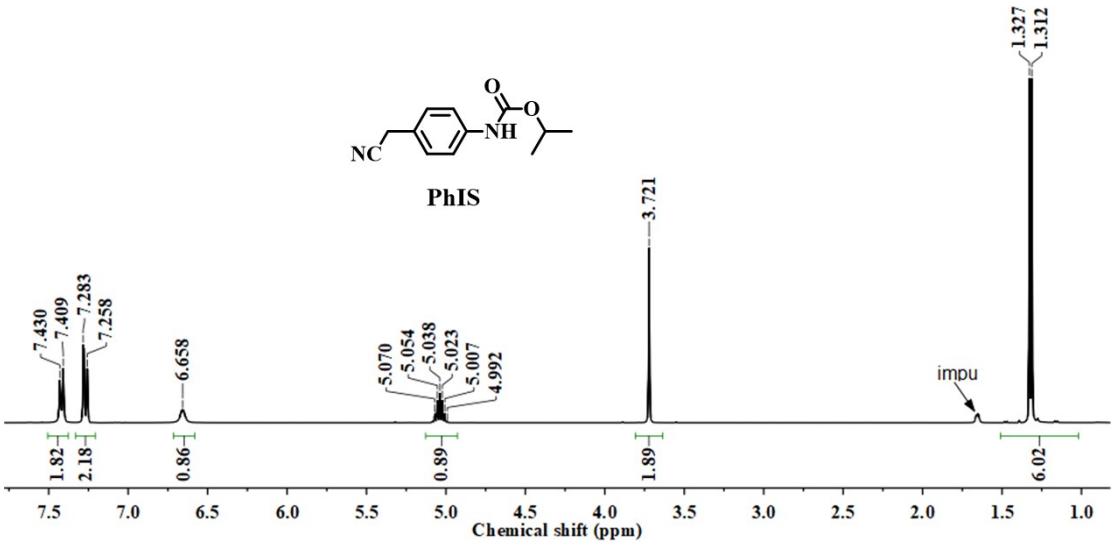

Fig. S15 The ^{1}H NMR spectrum of **PhIS** in the $CDCl_3$.

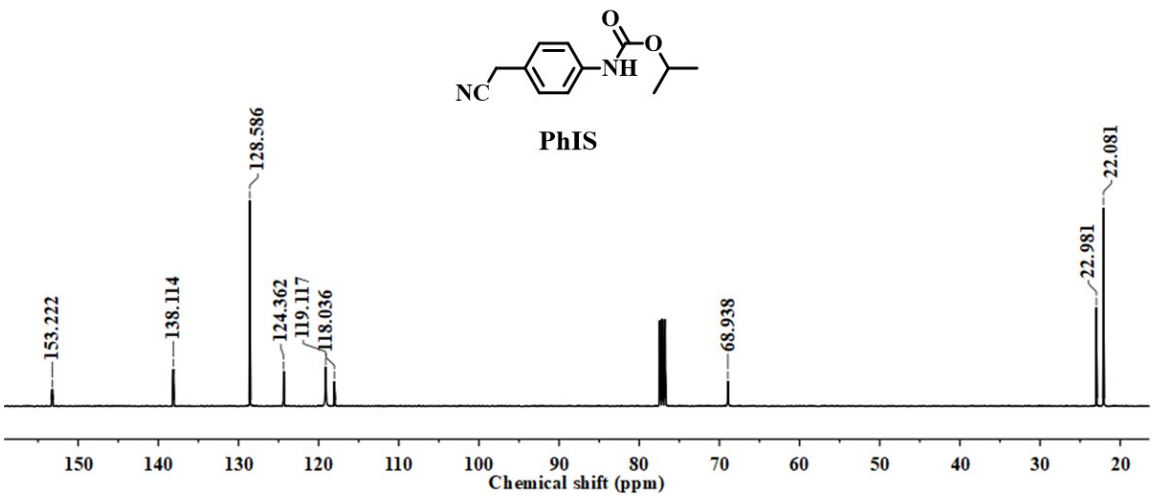

Fig. S16 The ^{13}C NMR spectrum of the **PhIS** in the $CDCl_3$.

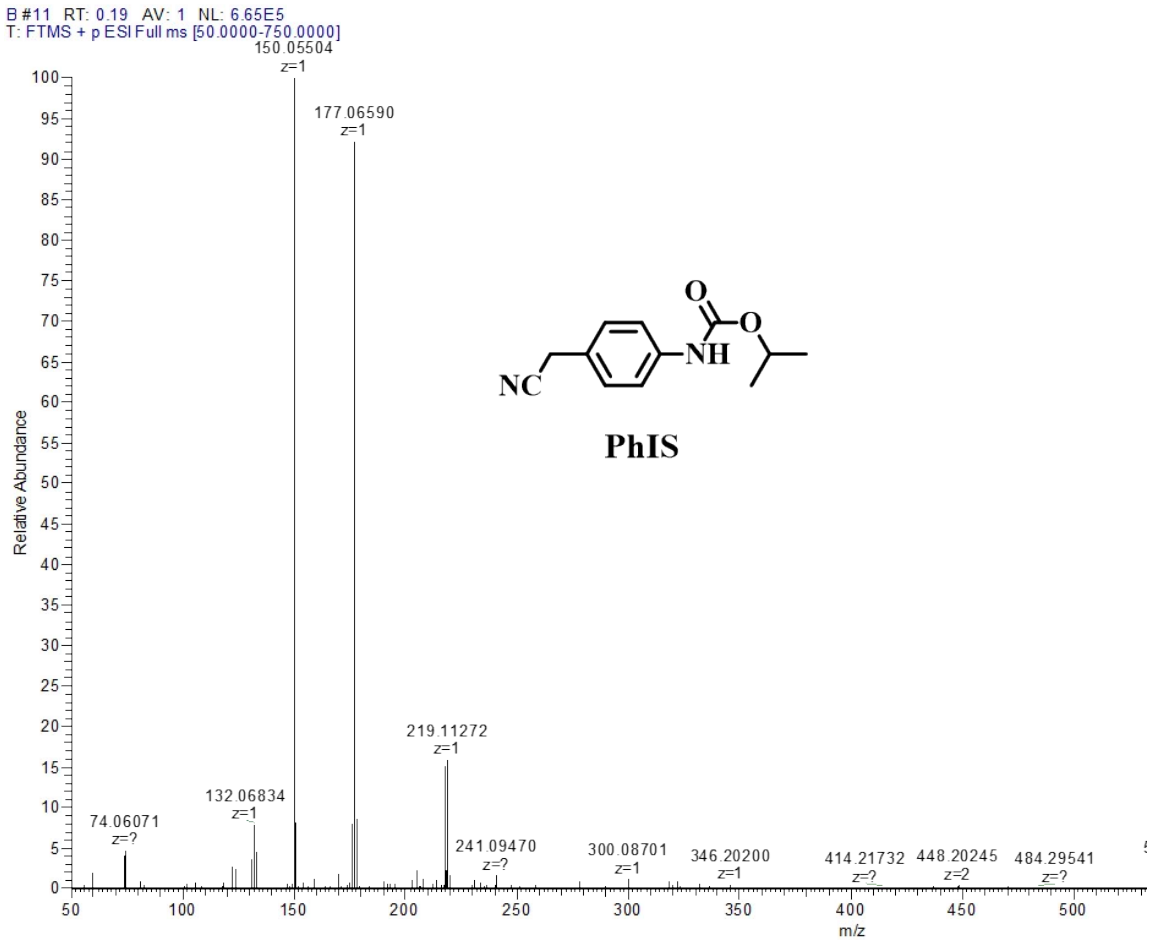

Fig. S17 The HRMS spectrum of the **PhIS**.

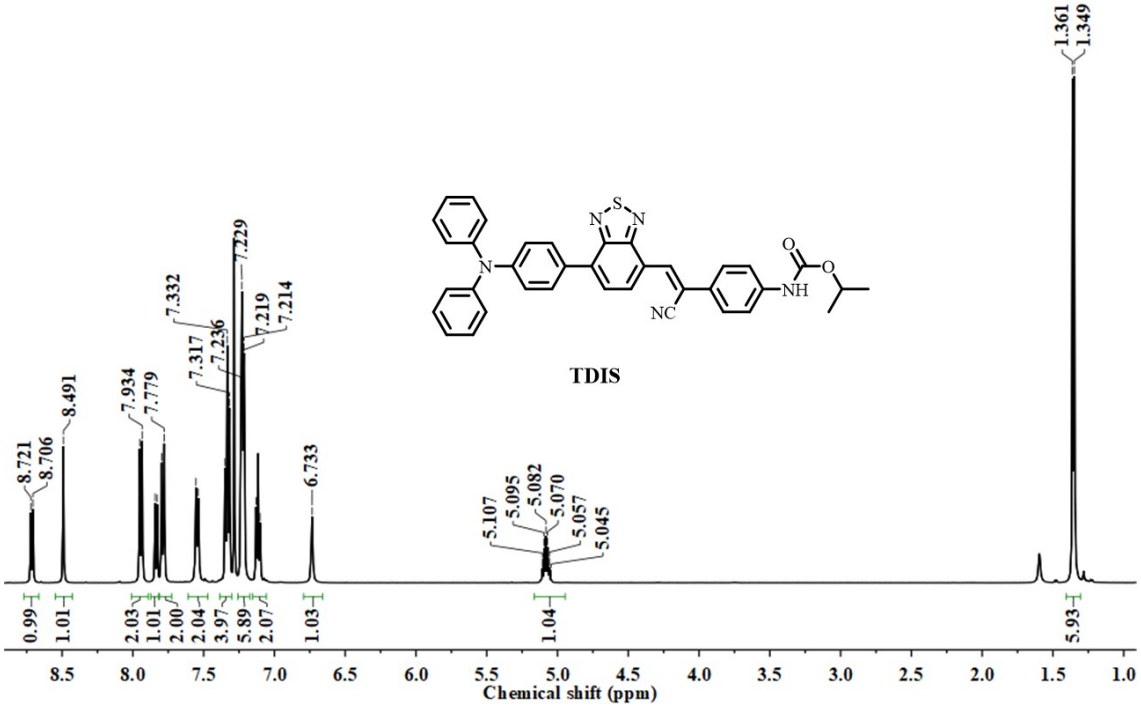

Fig. S18 The ^{1}H NMR spectrum of **TDIS** in the $CDCl_3$.

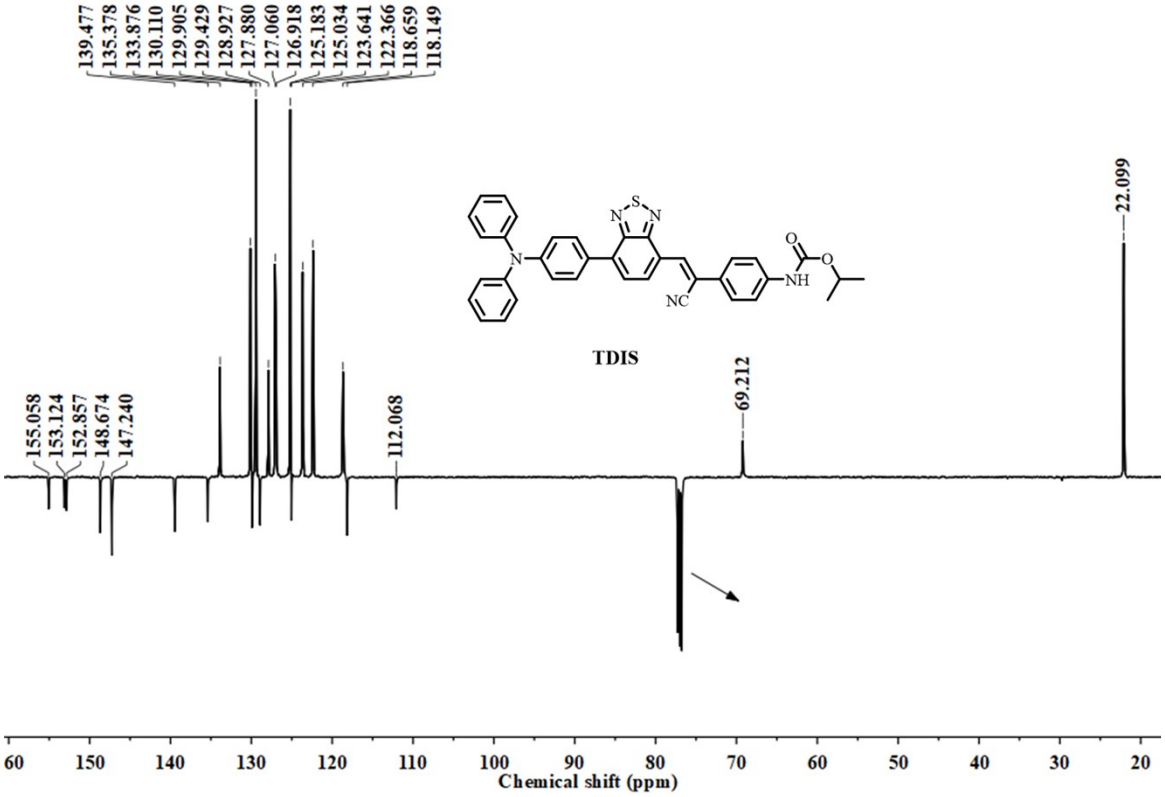

Fig. S19 The ^{13}C NMR spectrum of the **TDIS** in the $CDCl_3$.

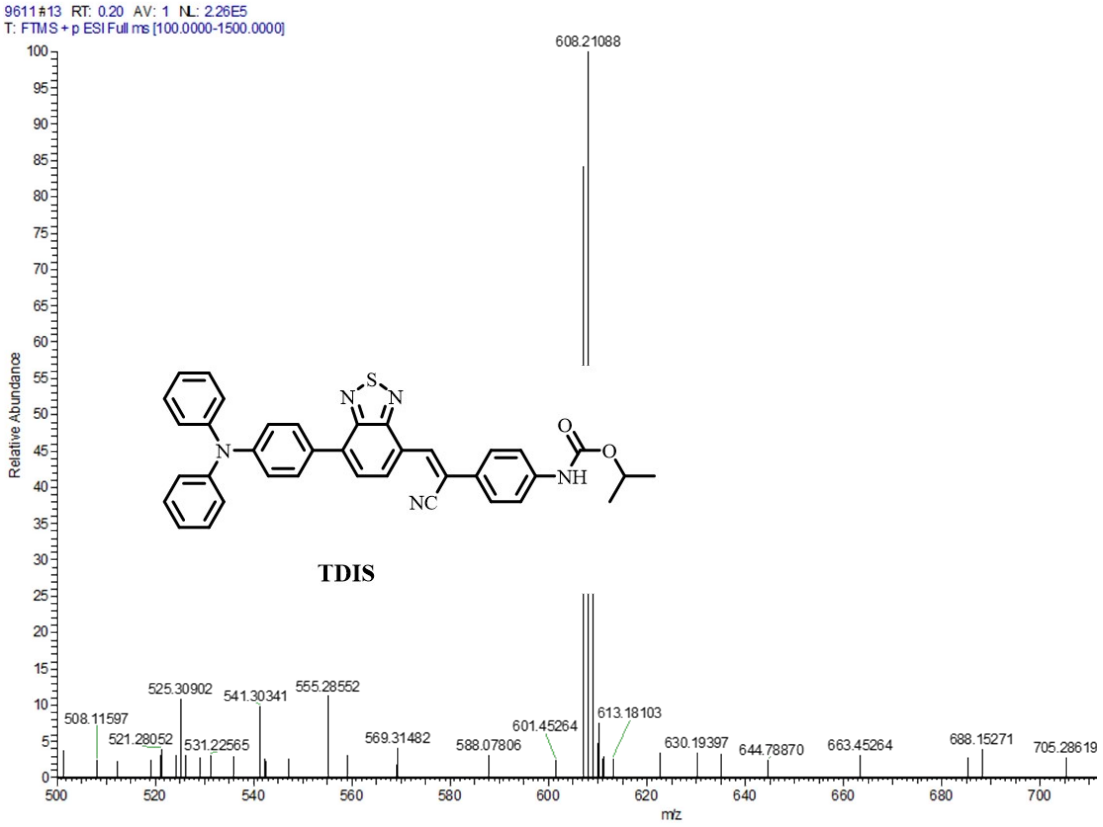

Fig. S20 The HRMS spectrum of the **TDIS.**